



Optimization of treatment efficiency of UV/H₂O₂ process on simulated textile industry wastewater

P. Manikandan^{a,*}, P.N. Palanisamy^a, R. Baskar^b, P. Sivakumar^a, P. Sakthisharmila^a

^aCentre for Environmental Research, Department of Chemistry, Kongu Engineering College, Perundurai, Erode 638052, TN, India, Tel. +91 9715508383; emails: manipal2k@gmail.com (P. Manikandan), aspavithran@gmail.com (P.N. Palanisamy), psivakumar3888@gmail.com (P. Sivakumar), sakthisharmila@gmail.com (P. Sakthisharmila)

^bDepartment of Food Technology, Kongu Engineering College, Perundurai, Erode 638052, TN, India, email: naturebaskar@yahoo.co.in

Received 21 November 2015; Accepted 24 March 2016

ABSTRACT

The present study involves optimization of UV/H₂O₂ process on a simulated dye bath effluent by varying initial H₂O₂ concentration, pollution load, and pH. The process was optimized by four factors and three levels of Box–Behnken design coupled with response surface methodology. During the experiment, color removal and degradation studies were also performed to ensure the treatment efficiency. The results obtained show that the color removal efficiency can be achieved within a short time due to the degradation of the structure which is more susceptible to oxidation. Then slower and gradual degradation of the simple and conjugated aromatic compounds takes place. In the first 5 min of the irradiation of the dyes, the pH value decreased from 11 to 9.5 and for another pH value decreased from 9 to 7.01. The drop in the pH value is mainly due to the formation of organic as well as inorganic acid as a degradation product. Under the optimum operating conditions such as pollution load of 64%, initial concentration of H₂O₂ 0.6 M, initial pH 8, and treatment time of 81 min the predicted removal efficiencies are 98.77 and 86.11% for Color removal and COD removal, respectively.

Keywords: UV/H₂O₂; Box–Behnken design; Color removal; COD; Effluent; Degradation

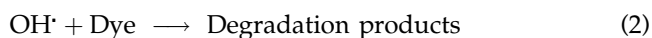
1. Introduction

Dyeing and finishing process of the textile plants produce high level of environmental contamination due to the high toxicity of the chemical components of the wastewater [1–3]. Azo dyes are the largest group of colorants to textile fabrics, which we mostly use for the production. These dyes contain one (mono azo), two (diaz), or more (polyazo) azo groups (–N=N–),

which are linked to aromatic rings. Natural fibers such as cotton and wool are dyed using reactive azo dyes. But such dyes possess low fixation rate and consume more water for preparation, dyeing, washing, and rinsing stages. Most of the unfixed dyes are discharged directly into the environment or after the partial treatment. Potentially carcinogenic aromatic amines may be produced by the metabolic cleavage of such complex dyes. Because of the complexity of the chemical structure, biological treatments are not efficient for the degradation.

*Corresponding author.

The uses of conventional oxidants for the treatment of dye wastewater are not always feasible owing to thermodynamic and kinetic limitations of the common reagents [4–6]. Advanced oxidation processes decompose the chromophore of the dye and consequently realize the complete decolorization. This can be possible by the generation of powerful hydroxyl radical with an oxidation potential of 2.80 V which can oxidize broad range of organic compounds. A direct method for the generation of the hydroxyl radical is hydrogen peroxide photo cleavage by means of UV_{254} radiation [7–11]:



The main objective of this investigation is to optimize the effect of UV/ H_2O_2 process on variable parameters such as initial pollution load, initial H_2O_2 concentration, and initial pH of the simulated wastewater on the color removal and COD removal. This study also concentrates on the degradation of aromatic, azo, and sulfonic functional groups in the dye. Finally the results were optimized using Box–Behnken experimental design with four factors and three levels of optimization for all the variables.

Table 1
Composition of the simulated dye bath effluent

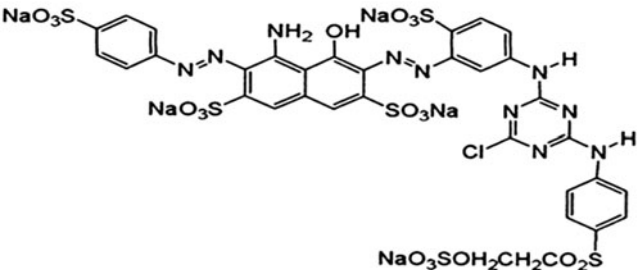
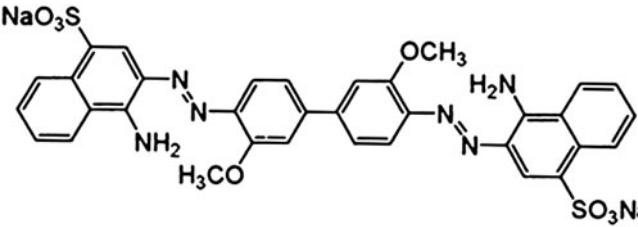
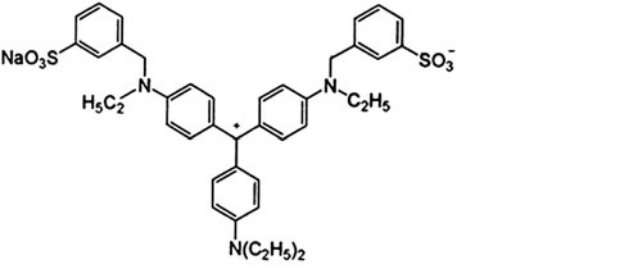
S. no	Constituents	Concentration (mg/L)	Structure of the dyes
1	Reactive blue	600	
2	Direct red	600	
3	Acid violet	600	
4	Starch	500	
5	Sucrose	500	
6	NaCl	5,000	
7	Na_2SO_4	1,000	
8	Na_2CO_3	1,000	
9	$NaHCO_3$	1,000	
10	Na_2HPO_4	500	
11	NaOH	1,200	
12	Detergent	300	

Table 2

Comparative physicochemical characterization of simulated dye bath effluent with real time effluent [12]

Parameters	Typical characteristics of real time textile effluents					
	Sruthi dyeing, Veerapandi Pirivu, Tiruppur	CETP, Veerapandi, Tiruppur	CETP, Mannarai, Tiruppur	CETP, Mannarai, Tiruppur	Texwel dyeing, SIDCO, Tiruppur	Simulated dye bath effluent
pH	9.04	9.31	8.15	10.08	9.03	10.68
Conductivity (mScm-1)	8.13	8.64	8.88	14.79	10.78	19.4
COD (mg/l)	1,580	780	1,210	1,460	1,380	2,794
TDS (mg/l)	8,180	7,100	6,1120	13,000	7,760	13,630
Alkalinity (mg/l)	3,225	1,550	1,475	7,250	1,675	2,500
Total hardness (mg/l)	4,200	1,280	3,885	2,590	1,295	11,315
Chloride (mg/l)	75	533	145	278	1,668	5,112
Sulfate (mg/l)	2,496	2,304	960	6,300	2,520	1,750

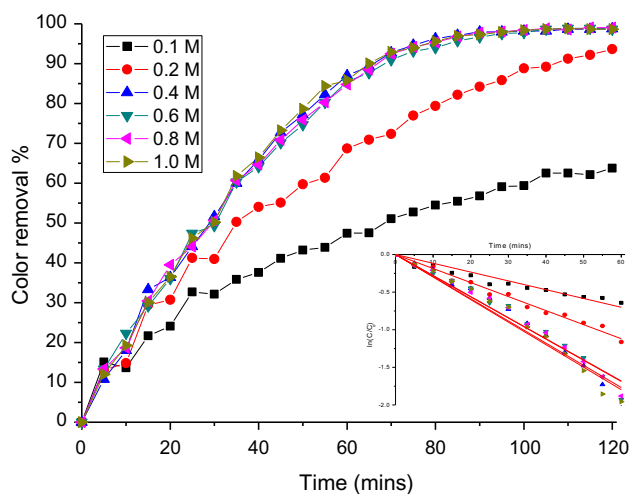


Fig. 1. Effect of initial concentration H_2O_2 with respect to time on color removal (at constant Pollution load = 60% and pH 7).

Table 3

First-order rate constants for the decolourization of simulated dye at the pollution load 60% and at the pH 7 in the presence of UV light

S. no.	Concentration of H_2O_2 (M)	R^2	k (min^{-1})	Color removal efficiency (%)
1	0.1	0.9115	0.0117	63.7602
2	0.2	0.9829	0.0186	93.6658
3	0.4	0.9616	0.0295	98.7705
4	0.6	0.9687	0.0280	98.6301
5	0.8	0.9762	0.0281	99.0728
6	1.0	0.9641	0.0300	98.6466

2. Materials and methods

2.1. Simulated dye bath effluent

The exact composition of the simulated dye bath effluent is given in Table 1. The dyes used are of commercial grade and used throughout the experiments without further purification in order to represent the actual dyeing conditions. The other chemicals were of analytical grade and supplied by Merck. The dye bath effluent was simulated by dissolving proper amounts of three commercial dyes and dye assisting chemicals in hot deionized water ($T = 70^\circ C$) which is a representative sample equivalent to the characteristics of real time effluent [12] (Table 2).

2.2. Photo reactor

Photoreactions were carried out in a glass photoreactor comprised of a quartz tube surrounded by a

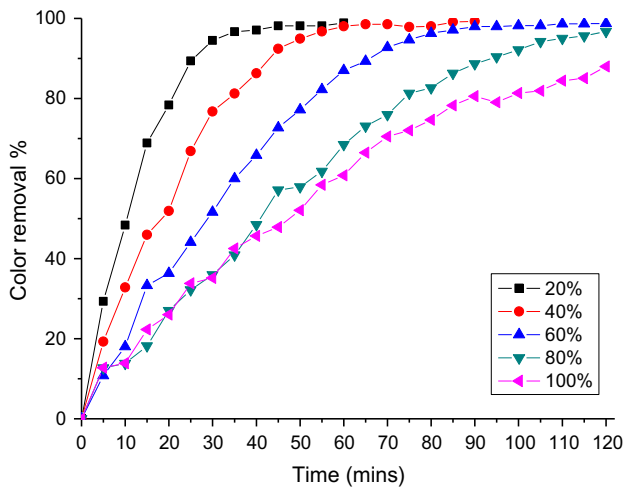


Fig. 2a. Effect of pollution load with respect to time on color removal (at initial concentration $\text{H}_2\text{O}_2 = 0.4 \text{ M}$ and $\text{pH} 7$).

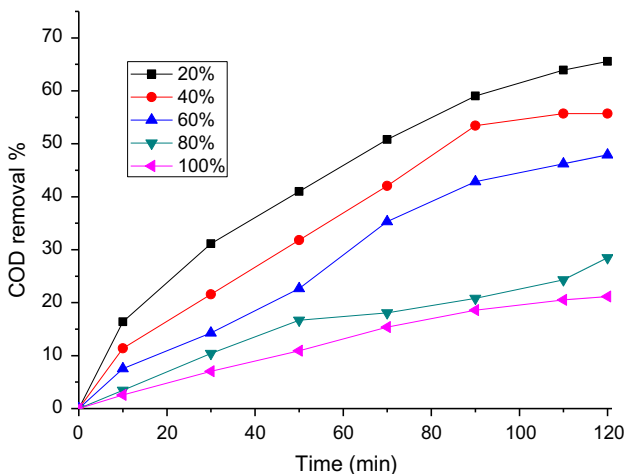


Fig. 2b. Effect of pollution load with respect to time on COD removal (at initial concentration $\text{H}_2\text{O}_2 = 0.4 \text{ M}$ and $\text{pH} 7$).

water cooling jacket and immersed in a Pyrex cylinder. The working volume of the photoreactor is 150 ml. The 16 W low pressure mercury vapor lamp with maximum emission at 254 nm is used as a source of UV irradiation.

2.3. Experimental procedure

Experiments were carried out with necessary quantity of the simulated dye bath effluent and H_2O_2 into the photoreactor. The solution was magnetically stirred and the temperature was maintained at 25°C by circulation of water in the cooling jacket. The pH of the solution was measured by pH meter and adjusted using dilute hydrochloric acid or sodium hydroxide. The samples were taken at definite time intervals to identify the loss of aromaticity of the dye during the photodegradation.

2.4. Analytical determination

The degradation of the effluent can be monitored using UV–visible spectrophotometer as a function of irradiation time at different wavelengths associated with simple aromatic (250 nm), aromatic carbonyl compounds (276 nm), conjugated dienes and/or polyaromatic (286 nm), and colored compounds (523 nm). Decrease in chemical oxygen demand (COD) and sulfur estimation were calculated to identify the mineralization rate. Standard analytical techniques were used as per the methods described by APHA [13].

3. Result and discussion

3.1. Effect of concentration of H_2O_2

The experiments were carried out in the presence and absence of UV irradiation. Color removal efficiency was less than 10% and no measurable removal efficiency was observed when it was carried

Table 4

Variation in first-order rate constants for the decolourization of simulated dye effluent with different pollution load and at 0.4 M initial H_2O_2 concentration, at the pH 7 in the presence of UV light

Pollution load (%)	Dye degradation kinetics					
	$R_{250 \text{ nm}}^2$	$k_{250 \text{ nm}} (\text{min}^{-1})$	$R_{276 \text{ nm}}^2$	$k_{276 \text{ nm}} (\text{min}^{-1})$	$R_{286 \text{ nm}}^2$	$k_{286 \text{ nm}} (\text{min}^{-1})$
20	0.9398	0.0152	0.9685	0.0219	0.9667	0.0293
40	0.9649	0.0106	0.9679	0.0208	0.9733	0.0256
60	0.9847	0.0098	0.9773	0.0161	0.9849	0.0205
80	0.8213	0.0051	0.9705	0.0117	0.9544	0.0138
100	0.9097	0.0069	0.9910	0.0102	0.9924	0.0122

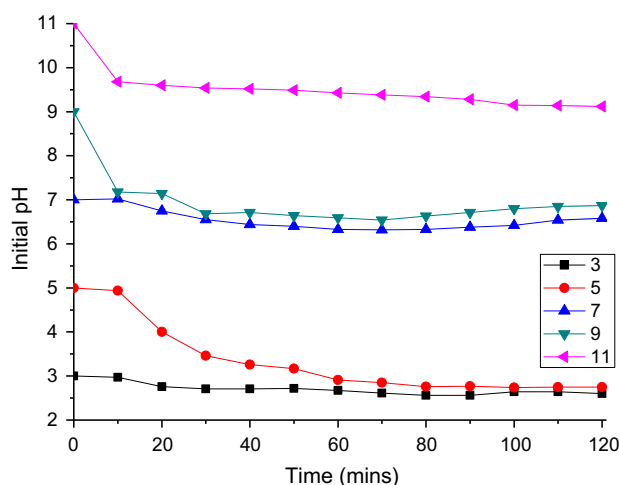


Fig. 3a. Effect of pH with respect to time (at initial concentration $H_2O_2 = 0.4$ M and pollution load = 60%).

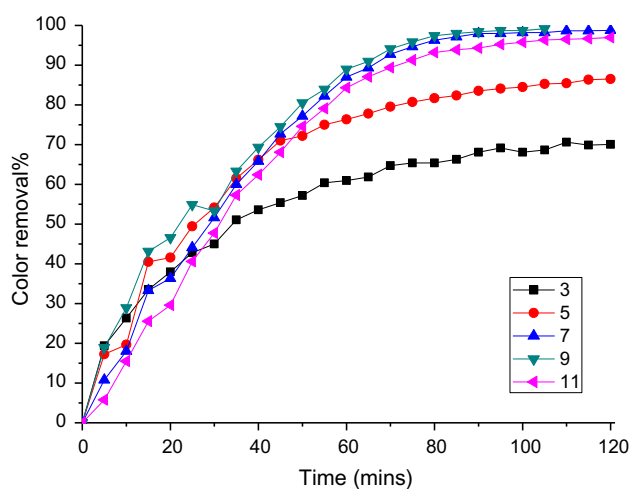


Fig. 3b. Effect of pH with respect to time on color removal (at initial concentration $H_2O_2 = 0.4$ M and pollution load = 60%).

out in UV and H_2O_2 individually, which was in agreement with the literature [14]. Notable removal efficiency was observed when it was treated with the UV/ H_2O_2 , it can be explained by the fact that the formation of powerful oxidant, OH^\cdot radicals by direct photolysis of hydrogen peroxide (Eqs. (1) and (2)). Due to the low molar absorptivity of the hydrogen peroxide, theoretically excess of hydrogen peroxide is needed to produce more OH^\cdot radicals [15]. So the efficiency of the degradation of the simulated effluent depends mainly on the concentration of the hydrogen peroxide. The concentration of hydrogen peroxide may either increase or decrease the degradation process. Therefore, it is essential to find out the optimum concentration of hydrogen peroxide for the better treatment efficiency. It was decided to conduct the experiment at the different initial concentration of hydrogen peroxide (0.1–1.0 M) and at fixed pollution load (60%) at pH 7 and at the temperature 25°C.

The first-order rate equation (Eq. (3)) can be represented by the following differential rate law:

$$r = \frac{-d[\text{Simulated dye}]}{dt} = k[\text{Simulated dye}]^0[H_2O_2] \quad (3)$$

The color removal efficiency (Fig. 1) increased from 63.76 to 98.77% with an increase in hydrogen peroxide concentration from 0.1 to 0.4 M. Lower color removal efficiency at 0.1 M is due to insufficient concentration of hydrogen peroxide for the generation of hydroxyl radicals. The quenching effect of hydrogen peroxide observed at higher concentration of hydrogen peroxide (from 0.6 to 1.0 M) leads to the lower color removal efficiency (Eqs. (4) and (5)):

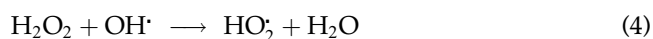


Table 5
Design summary for optimization

Factor	Name	Units	Type	Low actual	High actual	Low coded	High coded	Mean	Std. dev.		
A	Pollution load	%	Numeric	20	100	-1	1	60	25.731		
B	pH		Numeric	3	11	-1	1	7	2.573		
C	H_2O_2 load	Mole	Numeric	0.2	0.6	-1	1	0.4	0.129		
D	Time	Mins	Numeric	10	90	-1	1	50	25.731		
Response	Name	Units	Obs	Analysis	Minimum	Maximum	Mean	Std. dev.	Ratio	Trans	Model
Y_1	Color removal	%	29	Polynomial	16.23	98.9	67.184	23.259	6.094	None	Quadratic
Y_2	COD removal	%	29	Polynomial	7.05	86.07	47.479	22.919	12.209	None	Quadratic

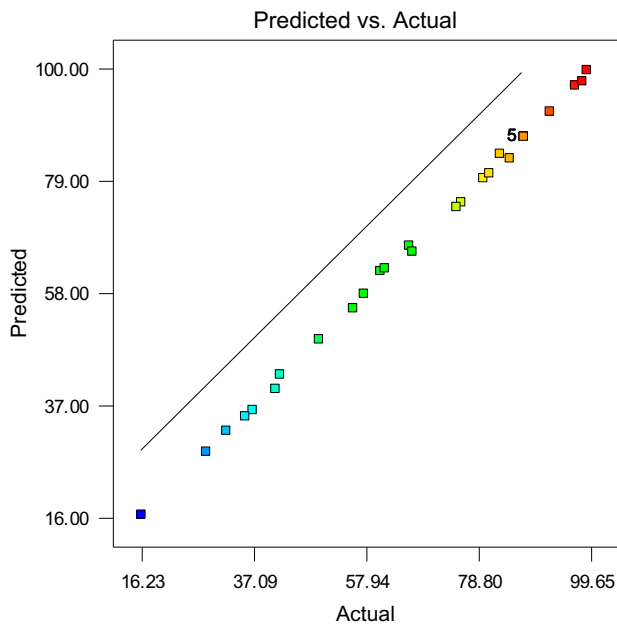


Fig. 4a. The actual and predicted Color removal Efficiency.

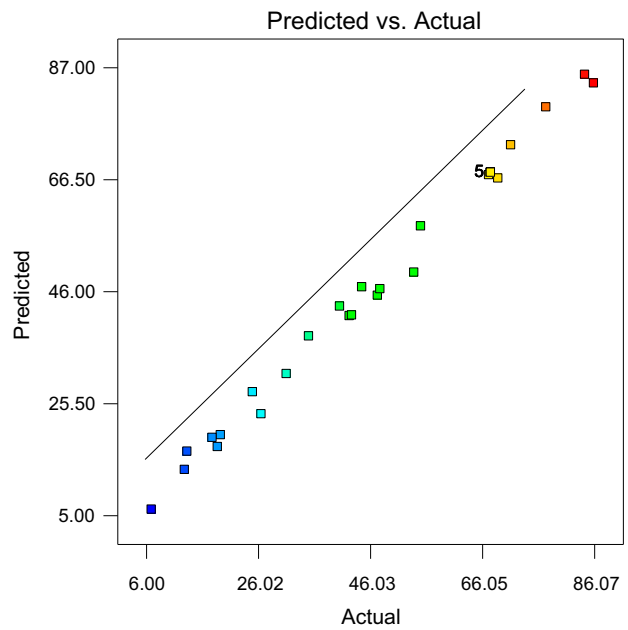


Fig. 5a. The actual and predicted COD removal percentage Efficiency.

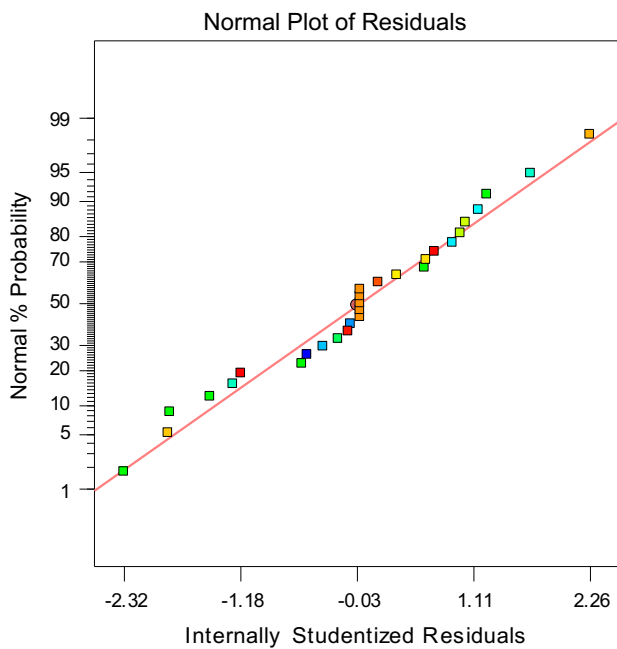


Fig. 4b. The studentized and normal percentage probability plot of Color removal Efficiency.

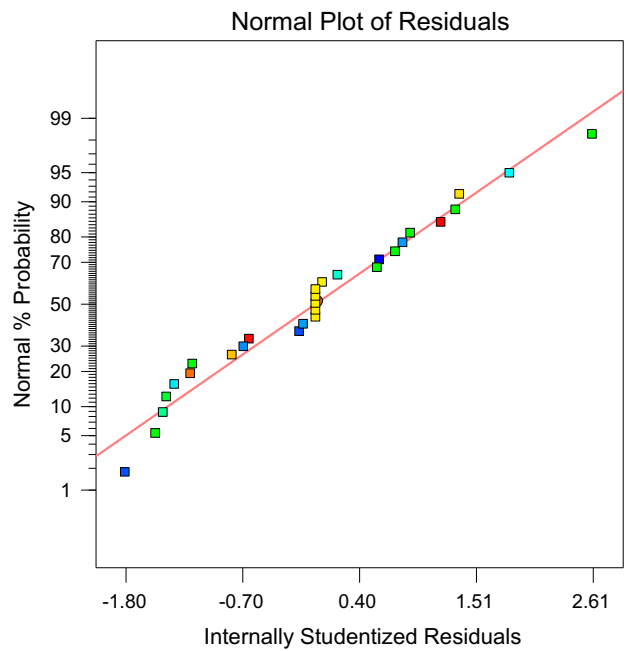
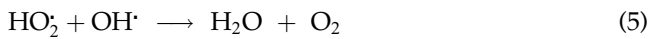


Fig. 5b. The studentized and normal percentage probability plot of COD removal Efficiency.



The correlation coefficient (R^2) values explain the fitting extent of the functional equation and the experimental data (Table 3). Higher rate constant value

(0.0295 min^{-1}) at the concentration 0.4 M shows the optimized conditions for the effective color removal efficiency of the process.

Table 6
Sequential model sum of squares of responses

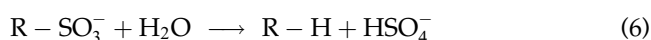
Source	For color removal				For COD removal			
	Sum of squares	Mean square	F-value	Prob. > F	Sum of squares	Mean square	F-value	Prob. > F
Mean	130,898.89	130,898.89			65,373.31	65,373.31		
Linear	12,178.12	3,044.53	20.82	<0.0001	11,095.45	2,773.86	16.09	<0.0001
2FI	464.08	77.35	0.46	0.8306	669.71	111.62	0.58	0.7421
Quadratic	3,031.87	757.97	766.66	<0.0001	3,364.79	841.2	113.66	<0.0001
Cubic	8.49	1.06	1.19	0.4286	90.23	11.28	5.06	0.0318
Residual	5.36	0.89			13.38	2.23		
Total	146,586.79	5,054.72			80,606.87	2,779.55		

3.2. Effect of pollution load

The effect of pollution load on the decolorization efficiency was monitored at different concentration level of pollution load and presented in Fig. 2a. The color removal efficiency was decreased with the increase in the pollution load from 20 to 100%. The molar absorption coefficient of the simulated dye at 254 nm is very high, so that an increase in the pollution load of the simulated dye effluent induces the internal optical density and the solution becomes highly impermeable to UV radiation. This may lead to decrease in the production of hydroxyl radicals and hence the removal efficiency is decreased.

In association with color removal efficiency, degradation kinetic behaviors were also analyzed for this condition to identify the extent of mineralization during the experiment. Table 4 shows the first-order kinetics for the dye degradation at different UV range such as 250, 276, and 286 as a function of time to the simulated effluent during the irradiation process. It was observed that fast decolorization occurs in the first few minutes of irradiation, which indicates the beginning of degradation with the structure more susceptible to oxidation such as azo groups. Then slower and gradual degradation of the simple and conjugated aromatic compounds take place until they attain a complete mineralization. Decrease in the COD removal efficiency during the irradiation process will also support the slower rate of dye degradation (Fig. 2b).

The formation of inorganic compounds leads to the formation of the sulfate ions, which is derived from organic sulfur (Eqs. (6) and (7)). The only product expected from the sulfur-containing dye is sulfite ion derived from the initial attack to the dye sulfonic groups [15]:



3.3. Effect of pH

Changes in the pH value of dye solutions as a function of the irradiation time for different initial pH values are shown in Fig. 3a. Within first 10 minutes of experiment initial pH value of the simulated dye bath effluent decreased from 11 to 9.5 and from 9 to 7.01. The drop in the solution pH is mainly due to the formation of organic acid as well as inorganic acids during UV irradiation of simulated dye bath effluent. But in neutral (pH 7) and in acid medium (pH 3–5) the decrease in initial pH takes place only after 10 min of time. Significant drop in the solution pH by nearly 2.5 pH units are probably due to the formation of low molecular weight organic acid as a degradation product when the initial pH of the simulated dye bath effluent is at pH 5. On the other hand, in neutral medium (pH 7) and in acidic medium (pH 3), weak organic acids were formed as a degradation product and hence no significant changes were observed [16,17].

The influence of pH on the rate of decolorization of the simulated dye bath solution by UV/H₂O₂ process was investigated at different pH values: 3.0, 5.0, 7.0, 9.0, and 11.0, using 60% pollution load solutions and 0.4 M H₂O₂ (Fig. 3b). The color removal efficiency was very less in acidic (pH 3), weak acidic (pH 5) and basic medium (pH 11), and it was more prominent in neutral (pH 7) and slightly basic medium (pH 9). The deactivation of OH· is more important when the pH of the solution is high. The reaction of OH· with HO₂⁻ is approximately 300 times faster than its reaction with H₂O₂. The scavenging effect [18,19] of inorganic anions present in the effluent (such as CO₃²⁻, SO₄²⁻, PO₄³⁻) decreased the color removal efficiency of the radicals at the pH 3–5.

3.4. Optimization

Statistical experimental design was employed to determine the effects of operating variables on color

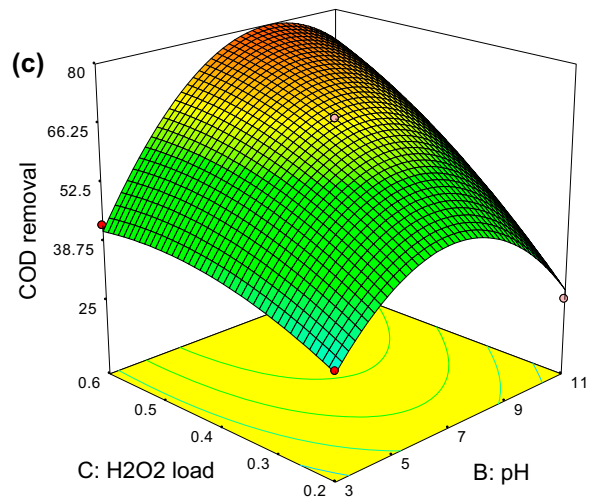
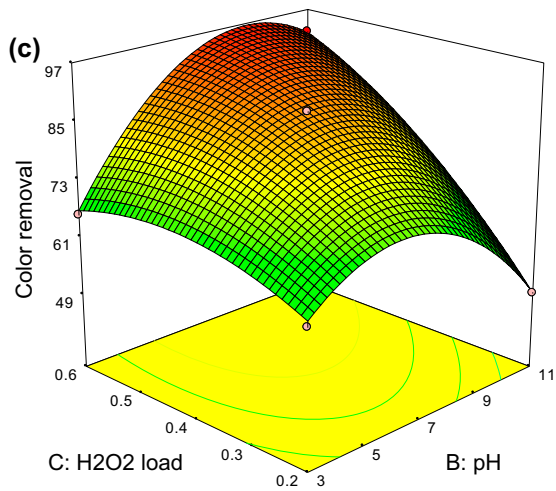
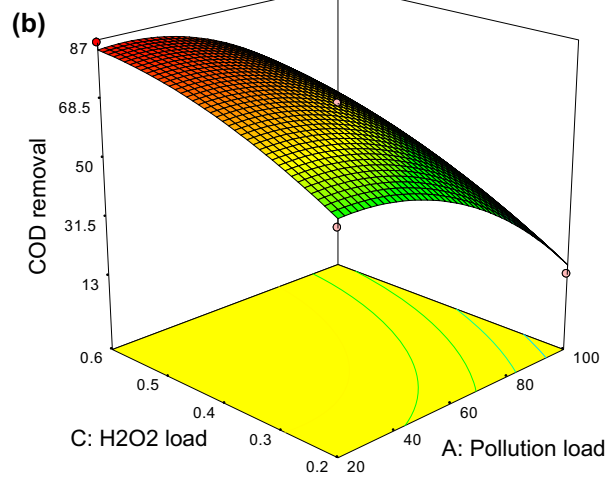
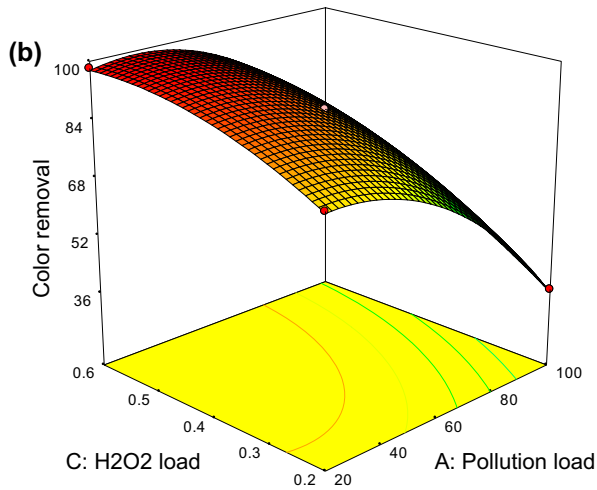
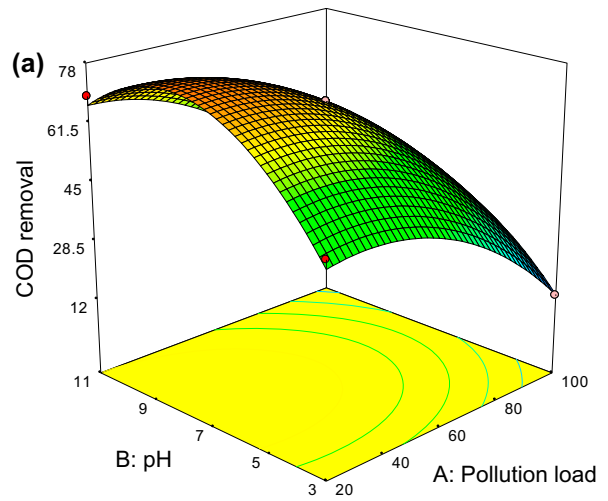
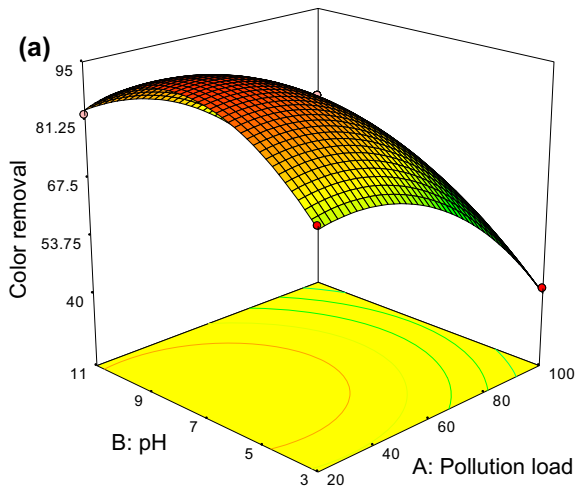


Fig. 6. a, b, c. 3D surface plot of Color removal vs. initial H₂O₂ concentration, Pollution load and pH.

Fig. 7. a, b, c. 3D surface plot of COD removal vs. initial H₂O₂ concentration, Pollution load and pH.

Table 7
Model summary statistics for response

Source	Color removal					COD removal				
	Std. dev.	R ²	Adj. R ²	Pred. R ²	Press	Std. dev.	R ²	Adj. R ²	Pred. R ²	Press
Linear	12.0930	0.7763	0.7390	0.7125	4,509.7096	13.1309	0.7284	0.6831	0.6403	5,478.843
2FI	13.0079	0.8059	0.6980	0.6424	5,609.8179	13.8812	0.7723	0.6458	0.5442	6,942.773
Quadratic	0.9943	0.9991	0.9982	0.9949	79.7259	2.7204	0.9932	0.9864	0.9608	596.7959
Cubic	0.9448	0.9997	0.9984	0.9508	771.1932	1.4934	0.9991	0.9959	0.8735	1,926.955

Table 8
ANOVA for responses

Source	For color removal				For COD removal			
	Sum of squares	Mean square	F-value	p-value	Sum of squares	Mean square	F-value	p-value
Model	15,674.0626	1,119.5759	1,132.4	<0.0001	15,129.9515	1,080.7108	146.03	<0.0001
A-pollution load	4,344.5491	4,344.5491	4,394.4	<0.0001	4,667.7241	4,667.7241	630.71	<0.0001
B-pH	103.8408	103.8408	105.03	<0.0001	579.491	579.491	78.302	<0.0001
C-H ₂ O ₂ load	1,645.7234	1,645.7234	1,664.6	<0.0001	2,344.4461	2,344.4461	316.79	<0.0001
D-Time	6,084.0033	6,084.0033	6,153.8	<0.0001	3,503.7919	3,503.7919	473.44	<0.0001
AB	10.0806	10.0806	10.196	0.0065	57.078	57.078	7.7125	0.0148
AC	38.502	38.502	38.944	<0.0001	3.2041	3.2041	0.4329	0.5212
AD	0.245	0.245	0.2478	0.6263	1.5625	1.5625	0.2111	0.6529
BC	367.6806	367.6806	371.9	<0.0001	296.5284	296.5284	40.067	<0.0001
BD	10.1761	10.1761	10.293	0.0063	243.36	243.36	32.883	<0.0001
CD	37.3932	37.3932	37.822	<0.0001	67.98	67.98	9.1856	0.009
A ²	973.9082	973.9082	985.07	<0.0001	889.8968	889.8968	120.24	<0.0001
B ²	1,367.941	1,367.941	1,383.6	<0.0001	2,537.9344	2,537.9344	342.93	<0.0001
C ²	162.3785	162.3785	164.24	<0.0001	146.223	146.223	19.758	0.0006
D ²	1,785.7118	1,785.7118	1,806.2	<0.0001	1,014.3921	1,014.3921	137.07	<0.0001
Residual	13.8413	0.9887			103.6104	7.4007		
Lack of fit	13.8413	1.3841			103.6104	10.361		
Pure error	0	0			0	0		
Cor total	15,687.9039				15,233.5619			
	Std. dev. = 0.99, C.V% = 1.48, Press = 79.73, R ² = 0.9991, Adj. R ² = 0.9982, Pred. R ² = 0.9949, AP = 116.19				Std. dev. = 2.72, C.V% = 5.73, Press = 596.80, R ² = 0.9932, Adj. R ² = 0.9864, Pred. R ² = 0.9608, AP = 40.68			

Table 9
Optimum operating conditions of the process variables for maximum color removal and COD removal

Solution no.	Pollution load (%)	pH	H ₂ O ₂ load (mole)	Time (min)	Color removal (%)	COD removal (%)	Desirability
2	64	8	0.6	81	98.77	86.11	1

removal efficiency and to find the combination of variables resulting in maximum color and COD removal efficiency. Three major steps in the optimization process involve: performing the statistically designed experiments, estimating the coefficients in a mathematical model, and predicting

the experimental outputs (as a response) and checking the suitability of the model. The minimum and maximum ranges for the four factors are illustrated in the Table 5. General form of a quadratic model for four variables is as given in Eq. (8) [20–23]:

Table 10
Comparison of dye removal efficiency of UV/H₂O₂ Process

S. no.	Dye	Concentration of the dye	Concentration of H ₂ O ₂	Time (mins)	% of Removal	Refs.
1	Reactive red 120	50 mg/L	20 ml/L	30	99.83	[26]
2	CI blue 13	100 ppm	0.67%	40	99.70	[27]
3	Reactive black 5	100 ppm	25 mM	60	99.00	[28]
4	Simulated dye bath effluent	64% Pollution load	0.6 M	81	98.77	Present Study
5	Direct yellow	100 ppm	10 mM	60	98.00	[28]
6	Reactive azo	1 × 10 ⁻⁴ M	10 mM	80	93.47	[29]
7	Acid blue 29	1 × 10 ⁻⁴ M	0.2 M	60	92.80	[30]
8	Direct red 28	100 ppm	50 mM	120	70.00	[28]
9	Vat green 01	100 ppm	0.5 g/L	140	45.00	[31]

$$\begin{aligned}
 Y = & \beta_0 + \beta_1 X_1 + \beta_2 X_2 + \beta_3 X_3 + \beta_4 X_4 + \beta_{11} X_1^2 + \beta_{22} X_2^2 \\
 & + \beta_{33} X_3^2 + \beta_{44} X_4^2 + \beta_{12} X_1 X_2 + \beta_{13} X_1 X_3 + \beta_{14} X_1 X_4 \\
 & + \beta_{23} X_2 X_3 + \beta_{24} X_2 X_4 + \beta_{34} X_3 X_4
 \end{aligned}
 \quad (8)$$

where Y = predicted response, β_0 = constant coefficient, $\beta_1, \beta_2, \beta_3,$ and β_4 = linear effect coefficients, $\beta_{11}, \beta_{22}, \beta_{33},$ and β_{44} = quadratic effect coefficients, $\beta_{12}, \beta_{13}, \beta_{14}, \beta_{23}, \beta_{24},$ and β_{34} = interaction effect coefficients, $X_1, X_2, X_3,$ and X_4 = independent variables.

For designing, analysis, and response surface were studied using Design-expert (stat-Ease, trial version) software. All the graphs presented were generated using this software. After fitting of Box–Behnken design (BBD) data, the final equation was derived in terms of Color removal and COD removal is given in Eqs. (9) and (10):

$$\begin{aligned}
 \text{COD removal \%} = & 67.65 - 19.72 A + 6.95 B \\
 & + 13.98 C + 17.09 D - 3.78 AB \\
 & + 0.90 AC + 0.62 AD + 8.61 BC \\
 & + 7.80 BD + 4.12 CD \\
 & - 11.71 A^2 - 19.78 B^2 - 4.75 C^2 \\
 & - 12.51 D^2
 \end{aligned}
 \quad (9)$$

$$\begin{aligned}
 \text{Colour removal \%} = & 87.20 - 19.03 A + 2.94 B \\
 & + 11.71 C + 22.52 D \\
 & - 1.59 AB + 3.10 AC \\
 & + 0.25 AD + 9.59 BC \\
 & + 1.59 BD - 3.06 CD \\
 & - 12.25 A^2 - 14.52 B^2 - 5.0 C^2 \\
 & - 16.59 D^2
 \end{aligned}
 \quad (10)$$

The model accuracy was checked by comparing the predicted and experimental oxidation efficiencies.

Figs. 4a and 5a shows the linear relationship between the predicted and experimental oxidation efficiencies. In this way, the residuals can be checked to determine how well the model satisfies the assumptions of ANOVA, and the internally studentized residuals can be used to measure the standard deviations separating the experimental and predicted values [24]. Figs. 4b and 5b shows the relationship between the normal probability (%) and the internally studentized residuals. The straight line means that no response transformation was required and there was no apparent problem with normality. According to Table 6, responses for Color and COD removal, the quadratic model was statistically significant ($p < 0.0001$) [25]. Figs. 6 and 7 show the 3D surface plots for the color removal and COD removal with respect to variable parameter (Tables 7 and 8).

3.5. BBD and their experimental results

The suitability of the optimized conditions for predicting the optimum response values was tested in the selected optimal conditions. Additional experiments using the predicted optimum conditions were carried out and the mean values were obtained from the experimental results were in agreement with the predicted values obtained from the model established (Table 9). These results compared with the results obtained from the previous researchers is given in Table 10.

4. Conclusion

The present study reveals that the treatment of efficiency of the UV/H₂O₂ method for the degradation of the simulated effluent/real time effluent. Strongly influencing parameters such as initial H₂O₂

concentration, pollution load, and initial pH were studied to identify the optimum condition for the maximum treatment efficiency. A BBD with the response surface methodology (RSM) was successfully applied to UV/H₂O₂ treatment system on the treatability of simulated dye bath effluent. The treatment efficiency of the process increases with an increase in the concentration H₂O₂ to the optimum value of 0.4 M, further increase in the concentration of H₂O₂ will reduce the treatment efficiency. The degradation process follows first-order kinetics with respect to the pollution load and the rate constant decreases with increasing pollution load. Variation in the initial pH also had a significant influence on the degradation efficiency. The maximum degradation efficiency was achieved in the neutral and slightly alkaline medium. Based on the statistical analysis (ANOVA), high coefficient of determining value (R^2) 0.9991 for color and 0.9932 for COD ensures a satisfactory fit of the second-order polynomial regression model with the experimental data. Additional experiments were carried out using the predicted optimum conditions and the values obtained were 98.01% for color removal and 85.26% for COD removal in agreement with the predicted values obtained 98.77% for color removal and 86.11% for COD removal.

Acknowledgement

The authors gratefully acknowledge the Department of Science & Technology (TSD), Government of India (Research Project no. DST/TSG/NTS/2012/67-G) for providing the financial support to carry out this research work and the experiments have been conducted at Centre for Environmental Research, Department of Chemistry, Kongu Engineering College, Perundurai, Erode – 638 052, TN, India.

References

- [1] A. Hamza, M.F. Hamoda, Multiprocess. Treatment of textile wastewater, in: Proceedings of the 35th Industrial Waste Conference, Purdue University, Lafayette, IN, 1980, pp. 151.
- [2] U. Pagga, D. Brown, The degradation of dyestuffs: Part II Behaviour of dyestuffs in aerobic biodegradation tests, *Chemosphere* 15 (1986) 479–491.
- [3] H.L. Sheng, M.L. Chi, Treatment of textile waste effluents by ozonation and chemical coagulation, *Water Res.* 27 (1993) 1743–1748.
- [4] K.G. Birchen, W. Lem, K.M. Simms, B.W. Dussert, Combination of UV oxidation with other treatment technologies for remediation of contaminated water, *J. Adv. Oxid. Technol.* 2 (1997) 345–441.
- [5] J.R. Boltan, S.R. Cater, Homogeneous photodegradation of pollutants in contaminated water: An Introduction, in: G.R. Helz, R.G. Zepp, D.G. Crosby (Eds.), *Aquatic and Surface Photochemistry*, EEUU, Lewis, Boca Raton, FL, 1994, pp. 467–490.
- [6] O. Legrini, E. Oliveros, A.M. Braun, Photochemical processes for water treatment, *Chem. Rev.* 93 (1993) 671–698.
- [7] H.Y. Shu, C.R. Huang, M.C. Chang, Decolorization of mono-azo dyes in wastewater by advanced oxidation process: A case study of acid red 1 and acid yellow 23, *Chemosphere* 29 (1994) 2597–2607.
- [8] C.G. Nambodri, W.K. Walsh, Ultraviolet light/hydrogen peroxide system for decolorizing spent reactive dye bath waste water, *Am. Dyest. Rep.* (1996) 15–25.
- [9] C. Morrison, J. Bandara, J. Kiwi, Sunlight induced decolouration/degradation of non-biodegradable orange II dye by advanced oxidation technologies is homogeneous and heterogeneous media, *J. Adv. Oxid. Technol.* 1 (1996) 160–169.
- [10] C. Galindo, P. Jacques, A. Kalt, Total mineralization of an azo dye (Acid Orange 7) by UV/H₂O₂ oxidation, *J. Adv. Oxid. Technol.* 4 (1999) 400–407.
- [11] G.M. Colonna, T. Caronna, B. Marcandalli, Oxidative degradation of dyes by ultraviolet radiation in the presence of hydrogen peroxide, *Dyes Pigm.* 41 (1999) 211–220.
- [12] P. Manikandan, P.N. Palanisamy, R. Baskar, P. Sivakumar, P. Sakthisharmila, Physico chemical analysis of textile industrial effluents from Tirupur city, TN, India, *Int. J. Adv. Res. Sci. Eng.* 4 (2015) 93–104.
- [13] APHA, Standard Methods For Examination of Water and Wastewater, American Public Health Association, WWA, Washington, DC, 2005.
- [14] N.H. Ince, M.I. Stefan, J.R. Bolton, UV/H₂O₂ degradation and toxicity reduction of textile azo dyes: Remazol black-B, a case study, *J. Adv. Oxid. Technol.* 2 (1997) 442–448.
- [15] M. Karkmaz, E. Puzenat, C. Guillard, J.M. Herrmann, Photocatalytic degradation of the alimentary azo dye amaranth, *Appl. Catal. B* 51 (2004) 183–194.
- [16] M. Styliidi, D.I. Kondarides, X.E. Verykios, Visible light-induced photocatalytic degradation of acid orange 7 in aqueous TiO₂ suspensions, *Appl. Catal. B* 47 (2004) 189–201.
- [17] Z. He, L. Lin, S. Song, M. Xia, L. Xu, H. Ying, J. Chen, Mineralization of C.I. reactive blue 19 by ozonation combined with sonolysis: Performance optimization and degradation mechanism, *Sep. Purif. Technol.* 62 (2008) 376–381.
- [18] G. Isil H.I. Nilsun, Degradation of reactive azo dyes by UV/H₂O₂: Impact of radical scavengers, *J. Environ. Sci. Health* 39 (2004) 1069–1081.
- [19] C.H. Liao, S.F. Kang, F.A. Wu, Hydroxyl radical scavenging role of chloride and bicarbonate ions in the H₂O₂/UV process, *Chemosphere* 44 (2001) 1193–1200.
- [20] M. Li, C. Feng, Z. Zhang, R. Chen, Q. Xue, C. Gao, Optimization of process parameters for electrochemical nitrate removal using Box–Behnken design, *Electrochim. Acta* 56 (2010) 265–270.
- [21] P. Tripathi, V.C. Srivastava, A. Kumar, Optimization of an azo dye batch adsorption parameters using Box–Behnken design, *Desalination* 249 (2009) 1273–1279.

- [22] F. Torrades, J. García-Montaña, Using central composite experimental design to optimize the degradation of real dye wastewater by Fenton and photo-Fenton reactions, *Dyes Pigm.* 100 (2014) 184–189.
- [23] K. Thirugnanasambandham, V. Sivakumar, Response surface modelling and optimization of treatment of meat industry wastewater using electrochemical treatment method, *J. Taiwan Inst. Chem. Eng.* 46 (2015) 160–167.
- [24] H.L. Liu, Y.R. Chiou, Optimal decolorization efficiency of reactive red 239 by UV/TiO₂ photocatalytic process coupled with response surface methodology, *Chem. Eng. J.* 112 (2005) 173–179.
- [25] N. Lavanyah, M. Thanapalan, Degradation of alizarin yellow R using UV/H₂O₂ advanced oxidation process, *Environ. Prog. Sustainable Energy* 33 (2013) 482–489.
- [26] R. Ananthashankar, A. Ghaly, Effectiveness of photocatalytic decolorization of reactive red 120 Dye in textile effluent using UV/H₂O₂, *Am. J. Environ. Sci.* 9 (2013) 322–333.
- [27] M.A. Jamal, M. Muneer, M. Iqbal, Photo-degradation of monoazo dye blue 13 using advanced oxidation process, *Chem. Int.* 1(1) (2015) 2–6.
- [28] U. Bali, E. Catalkaya, F. Sengul, Photodegradation of reactive black 5, direct red 28 and direct yellow 12 using UV, UV/H₂O₂ and UV/H₂O₂/Fe²⁺: A comparative study, *J. Hazard. Mater.* 114 (2004) 159–166.
- [29] M. Muruganandham, M. Swaminathan, Photochemical oxidation of reactive azo dye with UV–H₂O₂ process, *Dyes Pigm.* 62(3) (2004) 269–275.
- [30] I.A. Salem, H.A. Ghamry, M.A. Ghobashy, Catalytic decolorization of Acid blue 29 dye by H₂O₂ and a heterogeneous catalyst. Beni-Suef University, *J. Basic Appl. Sci.* 3(3) (2014) 186–192.
- [31] S.G. Schrank, J.N. dos Santos, D.S. Souza, E.E. Souza, Decolourisation effects of Vat Green 01 textile dye and textile wastewater using H₂O₂/UV process, *J. Photochem. Photobiol. A* 186(2) (2007) 125–129.